Radiocarbon (2025), pp. 1–16
doi:10.1017/RDC.2025.10137

Selected Papers from the 4th Radiocarbon in the Environment Conference, Lecce, Italy, 23–27 Sept. 2024

CONFERENCE PAPER

The potential of shells from *Mytilus edulis* for retrospective analysis of marine ^{14}C discharges from nuclear power plants

S. Bjarheim[1], K. Eriksson Stenström[1], A. Lindskog[2], M. Olsson[3], P. Carlsson[4] and S. Mattsson[5,6]

[1]Lund University, Department of Physics, Division of Particle and Nuclear Physics, Box 118, SE-222 21 Lund, Sweden, [2]Kristianstad University, Department of Environmental Science, Elmetorpsvägen 15H, SE-291 39 Kristianstad, Sweden, [3]Lund University, Department of Geology, Sölvegatan 12, SE-223 62 Lund, Sweden, [4]Lund University, Department of Biology, Division of Functional Ecology, Sölvegatan 37, SE-223 62 Lund, Sweden, [5]Lund University, Department of Translational Medicine, Medical Radiation Physics Malmö, Skåne and [6]University Hospital, SUS Malmö, SE-205 02 Malmö, Sweden
Corresponding author: K. Eriksson Stenström; Email: kristina.stenstrom@fysik.lu.se

Received: 04 December 2024; **Revised:** 22 May 2025; **Accepted:** 08 June 2025

Keywords: bivalve shells; marine environment; Mytilus edulis; nuclear power; radiocarbon; retrospective analysis

Abstract

Carbon-14 (^{14}C) is an important contributor to the collective effective dose to the public due to releases from nuclear power plants (NPPs). In Sweden, only airborne emissions of ^{14}C from NPPs are currently routinely monitored, and the existing data on waterborne ^{14}C discharges are limited. A recent study of ^{14}C in brown algae (*Fucus* spp.) in Swedish coastal waters showed higher $F^{14}C$ values collected at Ringhals NPP, on the Swedish west coast, than expected. Therefore, this study aimed at assessing if blue mussels (*Mytilus edulis*) could be used to retrospectively estimate the ^{14}C concentration of dissolved inorganic carbon (DIC) in seawater at three sites. A method was developed to extract the fibrous layer that forms visible annual structures in the shells. All samples were analyzed with accelerator mass spectrometry and the results compared with ^{14}C data from *Fucus* spp. For one of the analyzed shells (structures from 1974–1978), from the site Särdal, $F^{14}C$ in *Fucus* spp. and *M. edulis* agreed very well. For another shell (1972–1978), shell structures from some of the earlier years displayed up to 6% lower $F^{14}C$ than *Fucus* spp. $F^{14}C$ in one shell from a remote site, Båteviken, only had small annual variations (2017–2022: $F^{14}C = 1.070 \pm 0.015$ (1 σ)). Two shells from Ringhals NPP had higher average $F^{14}C$, and a significant temporal variability (2014–2022: $F^{14}C = 1.427 \pm 0.268$ (1 σ)). Difficulties in unambiguous identification of the annual structures in the shells, as well as the future potential of this method, are discussed.

Introduction

Despite being a weak beta emitter, with a long physical half-life of 5730 years, ^{14}C contributes to a significant part of the collective effective dose to the public from globally dispersed long-lived radionuclides emitted from the nuclear power industry (UNSCEAR 2016). Carbon is easily taken up by all living organisms, resulting in a certain amount of ^{14}C, e.g. in food. Hence, it is important to monitor airborne emissions as well as waterborne discharges of this radionuclide from the nuclear power industry.

The current regulations in Sweden regarding monitoring of radioactive emissions during normal operation of nuclear power reactors require, as far as possible and reasonable, nuclide specific measurements of airborne emissions and waterborne discharge of several radionuclides, including ^{14}C (SSMFS 2021:6). Airborne emissions of ^{14}C from Swedish nuclear power reactors are currently routinely monitored with the aid of commercial stack air samplers, followed by analysis with liquid scintillation counting (IAEA 2004). To our knowledge, only a few measurements have been performed

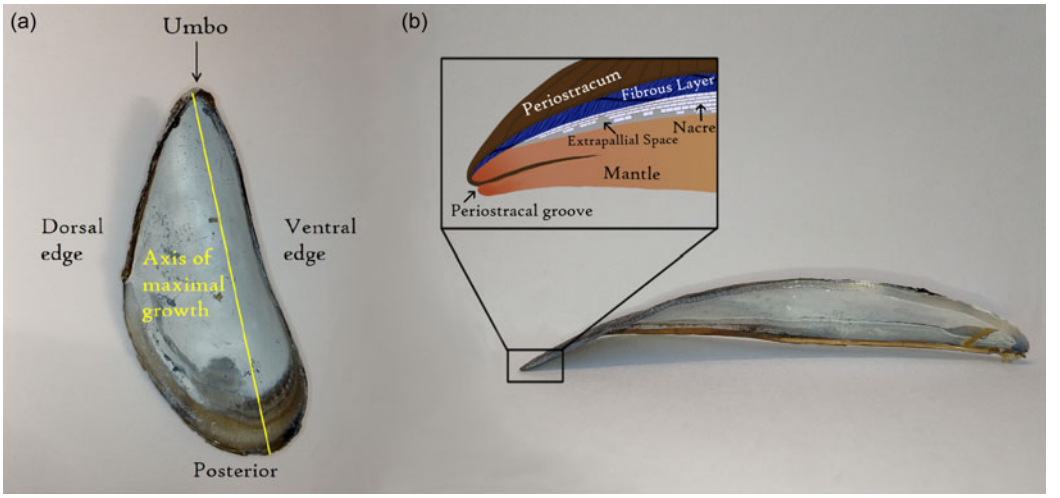

Figure 1. *(a). Terms used to denote parts of* Mytilus edulis. *(b) Illustration of the layers of a* M. edulis *shell where the mantle, a part of the soft tissue, is also included. The dark lines in the periostracum show the direction of the annual structures, while the bright parts show the direction of fiber growth. Based on figure 2 in* Checa (2018)*, recreated with permission from the author.*

on process water and liquid discharges (Magnusson 2007; Magnusson et al. 2008a, 2008b). These pointed to significantly lower liquid than airborne discharge rates, as also generally described by the IAEA (IAEA 2004). However, the excess of ^{14}C in the terrestrial and marine environment does not only depend on the amounts of ^{14}C in the gaseous and liquid waste streams. Airborne gaseous effluents of ^{14}C, released through high stacks, are effectively diluted before reaching biota at ground level. For liquid ^{14}C discharges the dilution is substantially less before reaching marine biota. Hence, biota in the local marine environment of a nuclear power plant (NPP) is relatively more exposed to discharged liquid ^{14}C, than biota in the terrestrial environment is exposed to gaseous ^{14}C releases.

In a previous study (Eriksson Stenström and Mattsson 2022), we investigated ^{14}C in samples of brown algae (*Fucus* spp.) from numerous sites along the Swedish coast in 2020. *Fucus* spp. are often used as bioindicators in environmental studies, as they are stationary (attached to rocks at the seabed) and concentrate many types of radioactive and non-radioactive pollutants (Mattsson et al. 2022). For ^{14}C, *Fucus* spp. reflect the current level of ^{14}C of Dissolved Inorganic Carbon (DIC) in the water. In the previous study (Eriksson Stenström and Mattsson 2022), *Fucus* spp. collected close to Ringhals NPP had up to ~25% excess of ^{14}C compared to that at nearby reference sites. This is a higher excess than what is normally found in the terrestrial environment of light-water cooled and moderated reactors such as the Ringhals NPP (Stenström et al. 2010). Due to the lack of previous measurements of ^{14}C in the marine environment of Ringhals NPP, we have investigated the possibility of retrieving such information by using the annual structures in blue mussels (*Mytilus edulis*), which are common in the waters along the Swedish west coast.

Mytilus edulis shells form annual structures as they grow (Figure 1). While there is conflicting information as to whether these structures form when the mussels are spawning, during summer, or due to slower growth during winter, there is a consensus that *M. edulis* shells form one band per year (Kautsky 1982). Observations by Seed (1969) strongly indicate that in *M. edulis*, the annual structures form during winter.

The ^{14}C in the *M. edulis* soft tissue reflects the amount of ^{14}C in its current food (the turnover time typically varies between 100 to 300 days depending on season (Smaal and Vonck 1997)). In the shells, ^{14}C mainly reflects DIC in the surrounding water during the whole growth period (Tierney 2017). *Mytilus edulis* are usually attached to a specific location by proteinaceous byssus threads, but can actively move using their foot, and also occasionally voluntarily detach from a location and drift with a

current or become involuntarily moved by waves (Ljunghager 2017). This semi-sessile characteristic lifestyle may partly limit their value as bioindicator (which preferably should be stationary).

There have been several past studies which have taken samples from annual structures in bivalves to study ^{14}C, however most were done on the species *Arctica islandica* to study the bomb pulse (Dunca et al. 2009; Schöne et al. 2005; Scourse et al. 2012). There have also been some studies where *M. edulis* shells have been used to investigate ^{14}C emissions from NPPs, but these studies have analyzed the entire shells and not the annual structures (Castrillejo et al. 2020; Tierney 2017). To the best of our knowledge, no studies have been published where *M. edulis* shells have been divided into annual samples for retrospective analysis of ^{14}C in the marine environment near NPPs.

On the other hand, the periodic growth patterns of bivalve shells, including *M. edulis*, has been used for analysis of $\delta^{13}C$, $\delta^{18}O$ and various elements such as Ba and Ca and applied to provide ecological and environmental data (Gillikin et al. 2006; Gröcke and Gillikin 2008; Surge and Schöne 2013). Parameters such as water temperature and precipitation can be revealed with sub-annual resolution by using advanced micro-growth extraction methods, such as microdrilling, micromilling and laser ablation techniques (Spötl and Mattey 2006). The carbon material of long-lived bivalves also has potential in environmental baseline monitoring (Steinhardt et al. 2016). E.g., records of metal pollution may be revealed in the shell annual structures (Steinhardt et al. 2016; Zuykov and Schindler 2019).

The aim of this study was to investigate the feasibility of *M. edulis* shells as bioindicators of past ^{14}C discharges as DIC from nuclear power plants. A comparison between the ^{14}C values in *Fucus* spp. and in annual structures of *M. edulis* shells was performed to evaluate how reliable the method using the annual bands of *M. edulis* shells is for estimating DIC at a specific location and time. The use of samples from the 1970s instead of contemporary samples is justified by the fact that the bomb pulse curve was steeper then. This provides a higher annual resolution in $F^{14}C$ compared to later years. An important requirement for the method developed, was that it should be possible to execute with the equipment already available at our laboratory. Furthermore, we wanted the method to be as simple as possible, to ensure it would be easy to reproduce. Micro-growth extraction methods, such as micromilling (Wurster et al. 1999) were for these reasons not possible.

Materials and methods

Mytilus edulis shell annual structures

We have implemented a method to extract ^{14}C from the fibrous layer of the annual structures of shells of *M. edulis* collected at the Swedish coast. Samples from Ringhals NPP as well as from a remote reference site (Båteviken close to the border of Norway) have been analyzed and compared to existing ^{14}C data in *Fucus* spp. from the same sites. We have also analyzed shells collected at Särdal on the Swedish west-coast in 1978 and compared the data to ^{14}C values in *Fucus* spp. from the same site and years 1972–1978 (Mattsson et al. 2022).

The annual structures in the nacre and the fibrous layer of a shell of *M. edulis* (Figure 1) form in different directions as compared to the curve of the shell valves (Checa 2018). The structure in the fibrous layer has thinner, threadlike fibers of calcite, while the nacre has a more brick-like structure of aragonite (Checa 2018). As a result of this, a sample containing both layers will have materials from more than one year. The two layers therefore need to be separated to ensure that the samples only contain material from one specific year. The fibrous layer was chosen, due to it being easier to divide according to its annual structures. A further discussion of this decision is found in Bjarheim (2024).

After removing the soft tissue from the *M. edulis* shells using a spoon and/or spatula, the annual structure of the shells was identified prior to dividing the shells into samples accordingly. The most widely used method for identifying the annual structures, thin sectioning (e.g. Clark 1980; Haag and Commens-Carson 2008; Neves and Moyer 1988), was avoided due to the carbon contamination risk from the use of epoxy. Instead, acetate peels were made to allow for the study of the internal structures of the shells. Acetate peels require less manual work and sample material compared to thin sections

(Kennish 1980; Lutz 1976). An acetate peel is produced by first cutting the shell along the axis of maximal growth, the cut edge is then sanded using a fine grit, before acetone is poured along the cut. Lastly the shell is placed on a cellulose film leaving an imprint of the edge. A full step by step description of the method used within this project can be found in Bjarheim (2024).

It was decided to divide the *M. edulis* shells according to their external annual structures, as this was practically the most achievable at this early stage of method development. The external annual structures were identified with the aid of a strong lamp. However, this method makes it difficult to differentiate between real annual structures and other disturbances. For example, a grain of sand trapped within the shell will result in the appearance of a darker area that can be mistaken for an annual band (Neves and Moyer 1988). Another issue is that the outer layer of the shell slowly erodes over time, predominately in the umbo region, thus removing the external annual bands. The external annual structures were compared with acetate peels made from the same shell, to identify false annual structures, as these will be less prominent internally.

To further ensure that age estimates of the *M. edulis* individuals were valid, the size of the *M. edulis* individuals was compared with growth curves from a nearby location (Dunca and Boalt 2011). Growth curves are based on the assumption that a species grows at a certain rate and reaches a maximum size. By then measuring the age and size of several specimens a graph showing the expected size at a certain age, for a specific species, can be made (Seed 1980). However, as noted by Seed (1980), individuals of *M. edulis* differ significantly in size depending on their growth conditions. Consequently, it is important to use relevant growth curves based on specimens found close to the sampling sites under investigation. It is also important to note that the *M. edulis* within a single settlement can vary in size even if they have the same age (Seed 1969), altogether making a large sample size preferable when making growth curves.

A common equation for such a growth curve, known as the von Bertalanffy growth equation, is

$$L_t = L_\infty \left(1 - e^{-kt}\right) + L_0, \tag{1}$$

where L_∞ is the maximum attainable length, k is a growth constant, t is the time, and L_0 is the length when the first annual band is formed (t = 0 in Figure 3, we later in manuscript denote this as age 1 year) (Dunca and Boalt 2011). Values of L_∞ and k can vary between sample sites. The software OriginPro 2024 (OriginLab, Northampton, Mass., USA) was used to fit the von Bertalanffy growth equations to plots of the length of the *M. edulis* shells as a function of the age of the mussel. The growth curves of the *M. edulis* individuals were compared to length data of *M. edulis* from Kullen (in Kattegat on the Swedish west coast, 56.3N, 12.4E), reported by Dunca and Boalt (2011). Additionally, data for *M. edulis* shells collected in the Baltic Sea (Högby fyr, 57.1N, 17.0E), with lower salinity than on the Swedish west coast, were used for size comparisons between different conditions (data from Dunca and Boalt (2011)). This method of combining acetate peels and growth curves for determination of the age of bivalves has also been used when studying other shells in the *Mytilus* family (Millstein and O'Clair 2001).

Sites

The relevant sampling sites along the Swedish west coast, and the location of the Swedish NPP Ringhals, are shown in Figure 2a. The site numbers 1 (Båteviken, 58.95N, 11.13E), 11 (Bua, at Ringhals NPP; 57.24N, 12.10E) and 15 (Särdal, 56.76N, 12.63E) are the same as in Eriksson Stenström and Mattsson (2022). Båteviken is located close to the border to Norway at about 220 km NNW of Ringhals NPP. At Bua (at Ringhals NPP), sampling was performed at two locations close to Krogstadsudde Lighthouse (57.24N, 12.10E): *Fucus vesiculosus* was collected ~70 m east of the lighthouse, while *M. edulis* was collected ~90 m south-west of the lighthouse (see Figure 2b). Further information summarizing some relevant aspects on airborne as well as liquid ^{14}C discharges from Ringhals NPP can be found in Eriksson Stenström and Mattsson (2022).

Särdal is situated about 65 km SSW of Ringhals NPP. The Särdal site is a reference site, which since 1967 has been used for regular sampling of mainly *Fucus* spp. for investigations of radionuclide

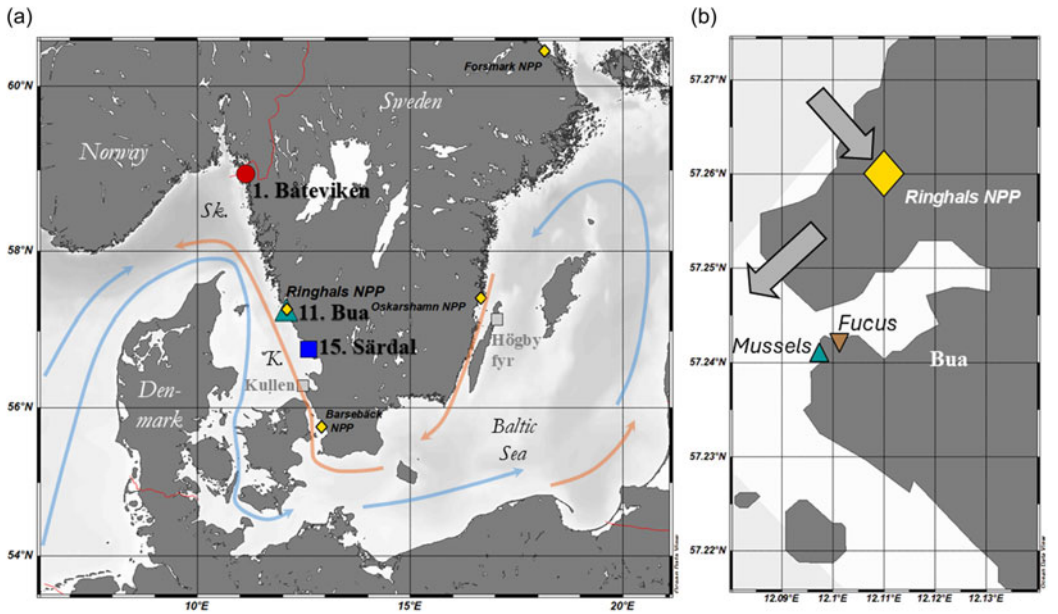

Figure 2. *(a) Map of southern Sweden including sampling sites and nuclear power plants.* Sk. – *Skagerrak,* K. – *Kattegat. Ocean currents are indicated (surface water movement in orange and bottom water movement in blue) (adapted from* Qiao et al. (2020) *and* Qiao et al. (2021)*). (b) Enlarged map of area surrounding Ringhals NPP. Arrows indicate inlet and outlet of cooling water. Maps: Schlitzer, Reiner, Ocean Data View, https://odv.awi.de, 2025.*

concentrations and metals (see Mattsson et al. (2022) and references therein). Two additional sites (not shown in Figure 2a, but located close to Båteviken), 52 Svinesund (59.10N, 11.27E) and 53 Saltbacken (59.08N and 11.23E) located at Ringdalsfjorden by the Norwegian boarder, were added to rule out contamination, especially at Båteviken, by discharges from the nuclear research reactor in Halden, Norway. Halden is located about 10 km further into the fjord from Saltbacken and about 10 km from Svinesund.

Sampling

Sampling of *Fucus* spp. was performed as described in Eriksson Stenström and Mattsson (2022), and *M. edulis* were collected in a similar manner by entering the water on foot. The *Fucus* spp. samples collected were constantly submerged in water to avoid uptake of atmospheric CO_2 (Cook et al. 2004). Several individuals of *M. edulis* and *F. vesiculosus* were retrieved at Båteviken on the 12th of October 2022. *Fucus vesiculosus* was also sampled at Båteviken at four other occasions: in spring 2020 (Eriksson Stenström and Mattsson 2022), autumn 2020, and spring and late summer in 2023. *Mytlius edulis* was collected at Bua by Ringhals NPP on the 12th of May 2023. At Bua, *F. vesiculosus* was sampled in spring (Eriksson Stenström and Mattsson 2022) and autumn 2020, in autumn 2022 and in spring and late summer 2023. The *M. edulis* and *F. vesiculosus* samples from Särdal were collected already on the 24th of December 1978, and have been stored in dried form in a biobank since the time of collection. Furthermore, *F. vesiculosus* was sampled on the 17th of May 2024 at Båteviken, Saltbacken and Svinesund. Water temperature and salinity were measured at the time of sampling of all marine samples (see Eriksson Stenström and Mattsson (2022)). Samples of grass, representing the terrestrial environment, were collected at Båteviken on the 12th of October 2022 and at Bua the following day.

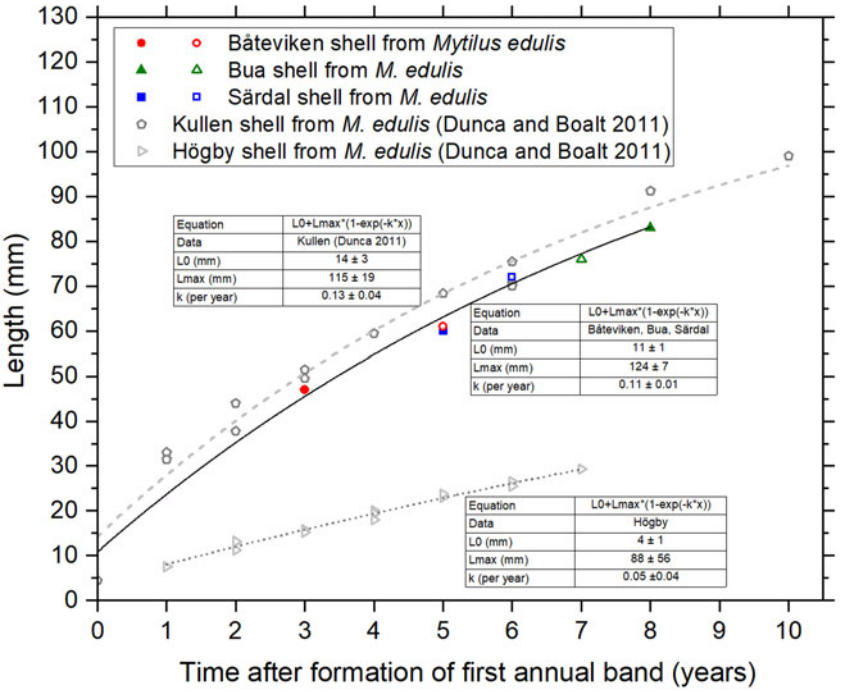

Figure 3. *Length of the six shells from* Mytilus edulis *analyzed (two individuals from each of the sites Båteviken (site 1), Bua (site 11) and Särdal (site 15) on the Swedish west coast) as a function of assessed age of the* M. edulis *individuals. The von Bertalanffy growth fit applied to the data is similar to that of age and length data of* M. edulis *from another site at the Swedish west coast, Kullen (data from Dunca and Boalt (2011)). The Högby* M. edulis *shell data (Dunca and Boalt (2011)), from* M. edulis *in the Baltic Sea, demonstrate the reduction in size of* M. edulis *in the Baltic Sea due to lower salinity.*

Sample preparation

The length and weight of the *M. edulis* individuals were measured (length 28-83 mm; typical weights from <1 g to a few g wet weight). For the 2022–2024 samples, the soft tissue was removed from the *M. edulis* shells, and frozen. Then the soft tissue was freeze-dried at – 55 °C for about 48 hours, before a sample was taken from the soft tissue of each shell and sent to the ^{14}C laboratory at Lund University. The sample from Särdal consisted of 14 *M. edulis* individuals. The soft tissue was removed from the shells and both the shells and soft tissue contents were dried in an oven at 65°C. The dry weight/wet weight ratio of the shells and contents were 94.8% and 16.3% respectively. Shells from 2 of the *M. edulis* individuals were used for analysis and the soft tissue content represented all 14 individuals.

When shining through the shells with a strong lamp, the annual structures appear as dark bands, as explained by Kautsky (1982). To better see the dark bands, the periostracum (the thin outer shell layer, see Figure 1b) was carefully sanded away beforehand. Each annual band was marked, using a marker with carbon-free ink, to keep track of their locations for later stages of the sample preparation. The *M. edulis* samples, two shells from each site, were then divided both according to the annual structures and according to the shell layers. After the shell layers had been separated through heating (see below), the pieces became very brittle and difficult to handle. Therefore, samples were divided according to the annual structures in the fibrous layer, before separating the latter from the nacre.

The first step in dividing the shell samples according to the annual structures was to cut off the dorsal and ventral edges using a lapidary saw. Then cuts were made along the annual structures, which were previously marked. When cutting out the annual structures, a Dremel tool with a diamond tipped saw blade rotating on a slow speed was used. Separating the fibrous layer from the nacre was then

accomplished by heating the cut samples. Each sample was placed in separate labelled beakers. After testing several different temperatures and durations, it was decided to heat the shell for ten minutes in an oven with air at 500°C, to achieve separation of the shell layers. Heating the shells for longer periods or at higher temperatures did not facilitate the separation, instead the shells became more brittle. What was left of the periostracum seemed to burn off at about 450°C, therefore a higher temperature than that was wanted. Furthermore, it was found that heating the shells for less than 10 minutes made the separation of the shell layers more difficult. The full process behind the method development, and a step-by-step instruction is found in Bjarheim (2024).

After being heated, the cut shell samples from the fibrous layer were subjected to standard sample preparation techniques used at the Lund Radiocarbon Dating Laboratory. The samples were thoroughly cleaned by brushing, and then put in an ultrasonic bath. Next, the shells were treated with a weak HCl acid, 10 ml 37% HCl diluted with deionized water to 1000 ml, to detach any organic material as well as nacre that might have been left on the fibrous layer. Shell weight before and after acid treatment is included in the Supplementary materials. The amount of acid was proportional to the weight of the sample (for further information, see Appendix B in Bjarheim (2024)). The solutions with the shell samples were put in an oven, with air at about 80°C, for three hours. Afterwards the shell samples were again thoroughly cleaned in an ultrasonic bath and then dried in a heating cabinet at 110°C.

Fucus spp. samples were dried in an oven at 70°C, ground and homogenized via mixing, prior to being cleaned with an acid-alkali-acid (AAA) pretreatment to remove carbonates and organic acids (Eriksson Stenström and Mattsson 2022). Grass samples were dried in air.

^{14}C analysis

The samples were analyzed using single-stage accelerator mass spectrometry (SSAMS) at the Radiocarbon Dating Laboratory at Lund University. Prior to graphitization in an AGE system (Wacker et al. 2010), CO_2 was liberated from the pretreated shell samples using phosphoric acid and *Fucus* spp. samples were combusted in an elemental analyzer. The resulting amount of graphite was ∼1 mg. The procedure for ^{14}C measurement is described e.g. in Skog (2007) and Skog et al. (2010). The background arising from sample preparation and the accelerator system was determined using IAEA-C1 marble. The standards used were IAEA-C7, IAEA-C8, SRM 4990B (OxI), and SRM 4990C (OxII). Raw data were analyzed at the Lund Radiocarbon Dating Laboratory. Results were expressed in terms of F^{14}C (Eriksson Stenström et al. 2011; Reimer et al. 2004). Reported uncertainties correspond to 1 σ.

Results and discussion

F^{14}C of all samples analyzed are presented in the Supplementary Material.

Growth curves

The estimated age of the *M. edulis* individuals that were subjected to shell analysis (2 from each site) were 6 and 4 years at Båteviken, 9 and 8 years at Bua, and 7 and 6 years at Särdal. The lengths of the mussels were between 47 mm and 83 mm (Figure 3). Figure 3 also includes data from Kullen on the Swedish west coast, obtained from Dunca and Boalt (2011). Kullen is located ∼310 km from Båteviken, ∼110 km from Bua, and ∼44 km from Särdal and is the closest site for which a growth curve for *M. edulis* was found in the literature.

The similarity in the fitted growth curves for the Kullen site and for the six *M. edulis* individuals from the sites Båteviken, Bua and Särdal demonstrates comparable growth conditions for *M. edulis* along the Swedish west coast. This conformity also strengthens the age estimates of our samples. Furthermore, Figure 3 highlights the size differences that can be observed within *M. edulis.* As shown, *M. edulis* individuals from Högby fyr, at the island Öland off the Swedish east coast, are much smaller than those

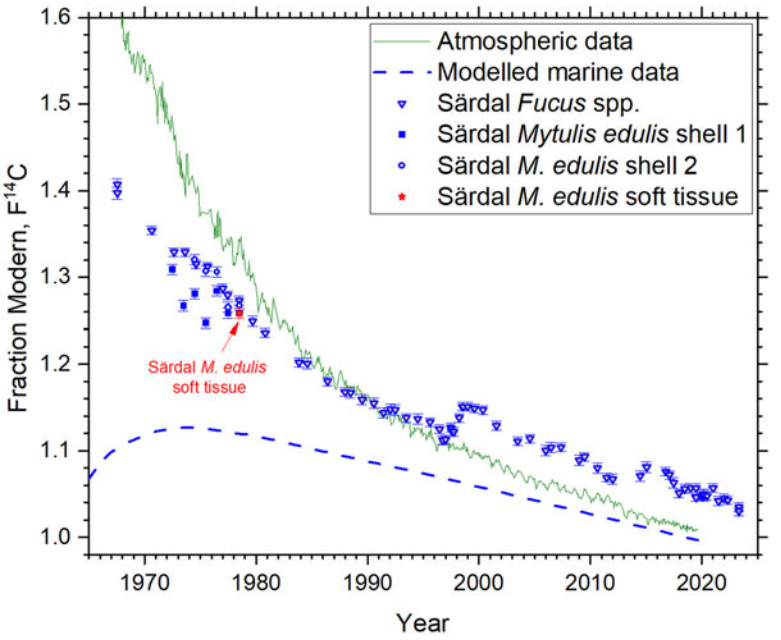

Figure 4a. *$F^{14}C$ in annual structures of the fibrous layer of two individuals of* Mytilus edulis *collected at Särdal (56.76N, 12.63E) in December 1978, average $F^{14}C$ in soft tissue of several individuals of* M. edulis *from the same site and sampling occasion, and $F^{14}C$ in* Fucus *spp. from the same site collected between 1972 and 1979 (Mattsson et al. 2025). The average formation season is plotted as summer for the* M. edulis *shell structures (dark ring forming in winter). The* Fucus *spp. data is plotted at the collection date. Atmospheric data are for Central European clean air CO_2 (Jungfraujoch, Switzerland) from Emmenegger et al. (2024), Conen et al. (2019), Hammer and Levin (2017), Levin and Kromer (2004) and Levin et al. (2013). The dashed curve shows the modelled global marine surface mixed-layer bomb pulse for the period 1950 to 1996 (Reimer et al. (2009), and values after this were extrapolated based on linear regression of marine data from 1987 to 1996. Uncertainty bars represent the analytical uncertainties (1 σ).*

from the west coast, due to the lower salinity of the Baltic Sea compared to the Kattegat and Skagerrak on the west coast. Methodological aspects and uncertainties regarding the age of *M. edulis* samples are further discussed below.

Särdal reference samples

The $F^{14}C$ data from the Särdal site is graphically summarized in Figure 4a, also including atmospheric ^{14}C data from the ICOS station Jungfraujoch in Switzerland (3580 m a.s.l) (Conen et al. 2019; Emmenegger et al. 2024; Hammer and Levin 2017; Levin and Kromer 2004; and Levin et al. 2013) and a modeled estimation of the global average $F^{14}C$ levels in the upper layer of the ocean (Reimer et al. 2009). The entire Särdal *Fucus* spp. data series (Mattsson et al. 2025; Eriksson Stenström and Mattsson 2022) is included in Figure 4a to demonstrate the influence of long-range transport of ^{14}C from the spent nuclear fuel reprocessing plants La Hague (France) and Sellafield (United Kingdom). The increase in $F^{14}C$ in *Fucus* spp. in Särdal in the late 1990s correspond to increased liquid ^{14}C discharges, mainly from La Hague, reaching the Swedish west coast after about 2 years (see Mattsson et al. (2025)). The general trend in *Fucus* spp. from Swedish west coast waters is that $F^{14}C$ increases towards the north (Eriksson Stenström and Mattson 2022). As previously reported (Eriksson Stenström and Mattsson 2022), the increase in $F^{14}C$ correlates positively with the increase in salinity towards the north of the

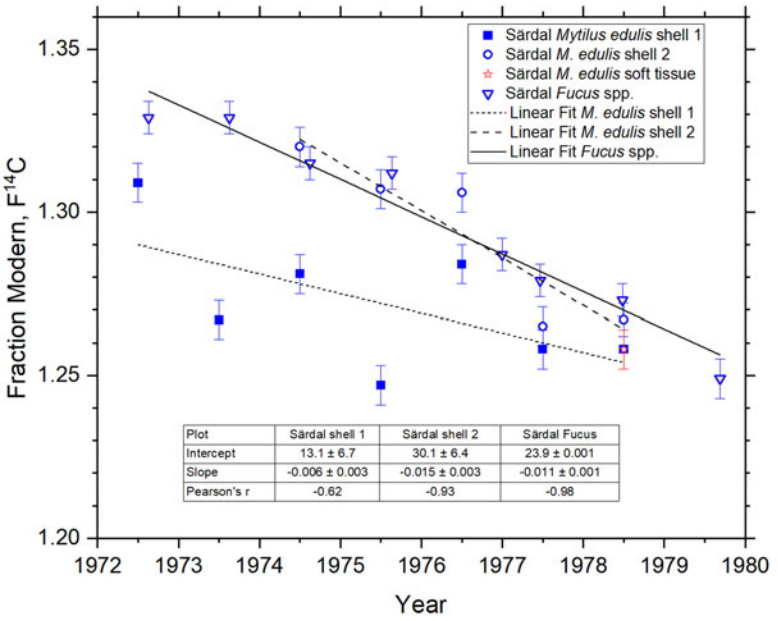

Figure 4b. *Enlargement of years 1972 to 1980 from Figure 4a. Uncertainty bars represent the analytical uncertainties (1 σ).*

Swedish west coast due to inflow of water of high salinity from the Atlantic, also carrying ^{14}C originating mainly from La Hague, but also from Sellafield.

The detailed results of the ^{14}C analysis of *M. edulis* collected at Särdal in 1978, and of *Fucus* spp. from the same site, are shown in Figure 4b. $F^{14}C$ of one of the shells (shell 2 in Figure 4) agrees well with $F^{14}C$ in *Fucus* spp. For the other shell (shell 1), $F^{14}C$ is generally lower (up to 5.2%) in the shell annual structures than in *Fucus* spp., in particular for the structures from 1972–1975. The lowered $F^{14}C$ in the four oldest annual structures of shell 1, compared to the more aligned $F^{14}C$ in shell 2 and *Fucus* spp., may indicate that this individual has moved from another habitat with lower $F^{14}C$ in DIC. For example, the specimen may originate from a place closer to the mouth of one of the three smaller creeks that open in the area and brings ^{14}C-depleted carbon into coastal waters (Lougheed et al. 2013), resulting in lower $F^{14}C$ in DIC at the creek mouth. $F^{14}C$ in the *M. edulis* soft tissue ($F^{14}C = 1.258 \pm 0.006$, average from several individuals, reflecting $F^{14}C$ in the dietary carbon of mussels) is identical to $F^{14}C$ in the annual band from 1978 in shell 2 ($F^{14}C = 1.258 \pm 0.006$), and overlapping within 1 σ to $F^{14}C$ in the annual band from 1978 in shell 1 ($F^{14}C = 1.267 \pm 0.005$). Hence, dietary carbon of *M. edulis* (represented by the soft tissue) and DIC (represented by the newer parts of the shell) appear to have been in equilibrium at Särdal at the time of sampling.

Båteviken

Figure 5 displays shell $F^{14}C$ data and $F^{14}C$ data from *F. vesiculosus* collected at Site 1 Båteviken at the northernmost Swedish west coast. The trend in $F^{14}C$ in the terrestrial environment in southernmost Sweden, obtained previously from analysis of tree rings and vegetation (Eriksson Stenström et al. 2022; Bernhardsson et al. 2023) is included, as well as $F^{14}C$ in terrestrial grass samples from Båteviken and from Bua (the latter close to Ringhals NPP). $F^{14}C$ in the terrestrial environment at both sites follows the trend line from southern Sweden, which also agrees well with central European data (Eriksson Stenström et al. 2022; Bernhardsson et al. 2023). Soft tissue from 3 *M. edulis* individuals collected in October 2022 has an average $F^{14}C$ of 1.058 ± 0.002, which is consistent with $F^{14}C$ from the annual

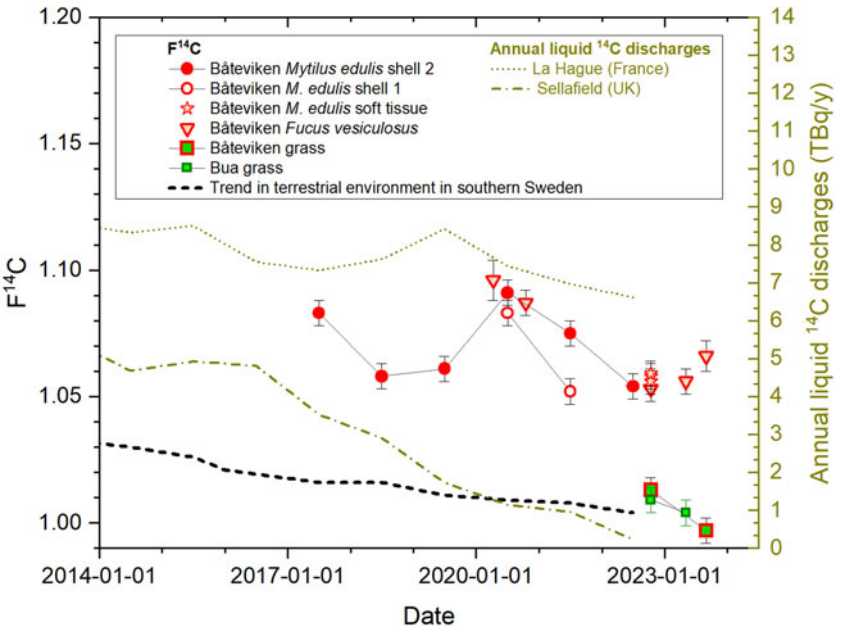

Figure 5. *$F^{14}C$ in annual structures from shells of* Mytilus edulis*, in soft tissue of* M. edulis *and in* Fucus vesiculosus *collected at Site 1 Båteviken (about 200 km NNE of Ringhals NPP). The average formation season is plotted as summer for the* M. edulis *shell structures (dark ring forming in winter). The $F^{14}C$* F. vesiculosus *data is plotted at the collection date. $F^{14}C$ in the terrestrial environment is represented by grass samples from the Båteviken (Site 1) and Bua (Site 11) (plotted at collection date). A trendline of $F^{14}C$ in the terrestrial environment of southern Sweden is also included (data from (Eriksson Stenström et al. 2022) and from (Bernhardsson et al. 2023)). Uncertainty bars represent the analytical uncertainties (1 σ). The right y axis displays annual liquid discharges from La Hague (France) and Sellafield (United Kingdom) (OSPAR 2012-2022).*

band for 2022 for Mussel 2 (1.054 ± 0.005). As for Särdal, the dietary carbon of *M. edulis* at Båteviken appear to be in equilibrium with DIC (represented by the outer band(s) of the shell).

As demonstrated in Figure 5, the marine environment (shells from *M. edulis* as well as *Fucus* spp.) at Båteviken has higher $F^{14}C$ in DIC than atmospheric CO_2 at the same site (represented by $F^{14}C$ in grass samples). For Båteviken, as for Särdal (Figure 4a), the main cause of this excess is believed to be long-range transport of ^{14}C from La Hague and Sellafield (Eriksson Stenström and Mattson 2022; Mattsson et al. 2025), but also other sources may occur, such as a contribution from Ringhals NPP (see below).

The peak in the shell data for 2020 may possibly be attributed to a peak in liquid discharges reported from La Hague in the year before (2019), see Figure 5 (OSPAR Commission 2024). We have previously estimated the transportation time from La Hague to Särdal (site 15) to about 2 years, hence the transport time to Båteviken should be less. At the Särdal site, we have previously also estimated a dilution factor of about 40 for La Hague and a dilution factor of 200 for Sellafield (transport time of about 4 years). Taking these estimates into account for Båteviken, the La Hague discharges would completely dominate compared to the discharges from Sellafield for the *M. edulis* individuals analyzed in the present study.

The *Fucus* spp. samples collected on the 17th of May 2024 at Båteviken, Saltbacken and Svinesund, to investigate the potential impact of the nuclear research reactor in Halden, Norway, showed that $F^{14}C$ decreased upstream in the fjord towards the reactor ($F^{14}C = 1.070 \pm 0.005$ at Båteviken, 1.058 ± 0.005 at Saltbacken and 1.038 ± 0.005 at Svinesund). As salinity decreased linearly with the $F^{14}C$ data upstream in the fjord (see Supplementary Material), discharges from the nuclear research reactor in Halden were ruled out as a significant source of ^{14}C on the Swedish west coast.

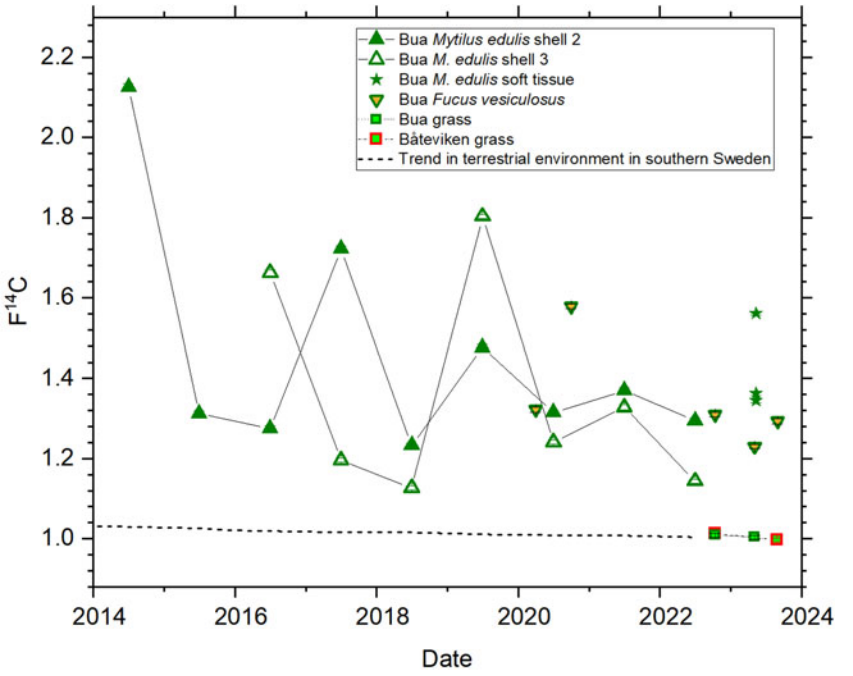

Figure 6. *$F^{14}C$ in annual structures from shells of* Mytilus edulis*, in soft tissue of* M. edulis *and in* Fucus vesiculosus *collected at Site 11 Bua (close to Ringhals NPP). The average formation season is plotted as summer for the* M. edulis *shell structures (dark ring forming in winter). The* F. vesiculosus *and* M. edulis *soft tissue data are plotted at the collection date. $F^{14}C$ in the terrestrial environment is represented by grass samples from the Bua (Site 11) and Båteviken (Site 1) (plotted at collection date). A trendline of $F^{14}C$ in the terrestrial environment of southern Sweden is also included (data from (Eriksson Stenström et al. 2022) and from (Bernhardsson et al. 2023)). Uncertainty bars represent the analytical uncertainties (1 σ).*

Bua at Ringhals NPP

The *M. edulis* (shell annual structures and soft tissue) and *F. vesiculosus* data for samples from Bua, located close to Ringhals NPP, is clearly influenced by water-borne discharges from the NPP (see Figure 6). Temporal variations in $F^{14}C$ are expected at the site. The mixing conditions of surface water of low salinity from the river Viskan (entering Kattegat <10 km south of the NPP), of low-salinity water from the Baltic Sea (in the surface water, usually flowing north) and of water with higher salinity from the North Atlantic (deeper water, usually flowing south) changes with time. Furthermore, local weather conditions (mainly wind) may result in frequent changes in the direction of the cooling water plume (also carrying the liquid radioactive discharges) from the NPP (Skoglund and Peterson 1988). The liquid ^{14}C release rates from the NPP may also change over time.

The expected temporal variations in $F^{14}C$ are clearly reflected in the *F. vesiculosus* samples. Also the annual structures of the *M. edulis* individuals show significant changes over the years. For the youngest 3 annual structures (2022, 2021 and 2020, see Figure 6), the two *M. edulis* shells analyzed display similar (but not identical) values in $F^{14}C$ (shell 2 is 13%, 3% and 6% higher than shell 3). For most of the earlier years, differences in $F^{14}C$ are pronounced for the two shells. The *M. edulis* individuals may, voluntarily or involuntarily, have changed habitat, or have had different temporal growth patterns. It should be noted that the *F. vesiculosus* data and the *M. edulis* data are not completely comparable, as the samples were collected about 150 m apart. Nonetheless, both sites are about 1.2 km from the outlet of cooling water from the NPP.

Another possibility is that the acid pretreatment may result in unrepresentative samples. Varying degrees of material may be removed from the surface and edges of the shell during acid pretreatment. The edges of the cut shell annual pieces represent the winter months. Hence, material from the winter months may be totally lost during the acid treatment. Additionally, if $F^{14}C$ in DIC in the surrounding water varies over the year, depending on fluctuating ^{14}C discharge rates, water currents and dispersion patterns, the removed material has a potential to give rise to an unrepresentative annual average $F^{14}C$ value. The degree of shell material removal (ARF, acid removal fraction) varied between 6% and 29% for the cut annual samples of the two shells from Bua (see Supplementary material). For each year, the absolute difference between the ARFs ($\Delta ARF = abs(ARF_{shell\ 2} - ARF_{shell\ 3})$) and the absolute difference between their $F^{14}C$ values ($\Delta F^{14}C = abs(F^{14}C_{shell\ 2} - F^{14}C_{shell\ 3})$) have been calculated (see Supplementary material). The largest difference in $F^{14}C$ for the cut annual samples of two shells from Bua is for 2017 ($\Delta F^{14}C = 0.536 \pm 0.009$). This year also has the largest difference in weight removal ($\Delta ARF = 23\%$). The opposite is valid for 2021: equal weight removals ($\Delta ARF = 0\%$) correspond to a low $\Delta F^{14}C$ (0.042 ± 0.008). The data is not conclusive but should be seen as an indication that the acid treatment may skew the results. However, the acid treatment procedure may not be necessary when preceded by the heating step. For most of the years with a large disagreement between samples, one of the shell pieces weighed less than 80 mg, therefore the sample weight could also be a factor of uncertainty. Despite this, since sample weight is related to the annual shell growth it cannot be controlled.

One further observation is that $F^{14}C$ in soft tissue of one the three individuals of *M. edulis* is significantly higher than the other two, despite being collected at the same site. Changes of habitat, or possibly different dietary conditions, may be the reason. This observation demonstrates that it is suitable to analyze not only one individual but several from the same site (individually or in a pooled sample).

It should also be noted that Ringhals NPP has had two more operational reactors apart from the two pressurized water reactors (PWRs) in current operation. One reactor was closed in 2019 (a PWR) and the other in 2020 (a Boiling Water Reactor, BWR), which implies a reduction in operationally discharged ^{14}C.

As a final note on the data from Bua, the grass samples from this site show no elevated levels of ^{14}C in the terrestrial environment. The site is, however, not in the main downwind direction from the stacks of the NPP. Furthermore, the two operational reactors at Ringhals NPP are PWRs, which are known to release ^{14}C to air mainly as hydrocarbons (thus not directly accessible to vegetation by photosynthesis) (IAEA 2004).

Methodological aspects and estimations of Mytilus edulis ages

In the determination of the age of mussels, growth curves are valuable as a complementary tool to the counting of annual structures. Ideally, individual growth curves from each sampling site would be preferred to ensure that size comparisons are made for as identical growth conditions as possible. As previously mentioned, growth curves assume that there is a maximum size that a species cannot surpass, it is however debated whether this is actually true for *M. edulis* (Seed 1980). Seed (1980) states that while there is some evidence for asymptotic growth, old mussels from a site with poor conditions will start growing more rapidly if they are placed in more favorable conditions. In the current study, growth curves have mainly been used as a further validation for the total age of the *M. edulis* individuals collected. Notably, the growth curves were not used to find the location of specific annual structures. Our estimates agree fairly well with the growth curve for *M. edulis* from Kullen, implying that the true age is indeed close to the age assessed from the identification of annual structures.

The largest challenge when locating the annual structures in the shell of *M. edulis* is to discern between true annual structures and other disturbance lines. As mentioned above, if a small particle is trapped within the shell it will appear as a darker section, which can resemble an annual band (Neves and Moyer 1988). Moreover, in contrast, Neves and Moyer (1988) noted that annual structures may be missing due to erosion of the fibrous layer. While most erosion will occur in the older region of the shell,

by the umbo, particles are more likely to get trapped within the younger regions, towards the posterior edge of the shell. From this it would be natural to assume that the lowest uncertainties about the location of the annual structures would be in the middle region. However, in the acetate peels made during this project the middle region of the shell were often difficult to analyze visually. Hence, in this pilot study, the uncertainties related to the locations of annual structures are most prominent in the middle regions of the *M. edulis* shells. The quality of the acetate peels could most likely be improved by adjusting and refining the technique specifically for preparation of *M. edulis* samples.

The acetate peels revealed that if the *M. edulis* individuals were collected early in the growth season the youngest annual ring was easily missed when externally identifying the annual structures, as it had only grown a few millimeters at this time. Consequentially this led to the shell samples from the youngest part of some shells containing a narrow band of material from the current growth season in addition to the material from the preceding year of growth. The youngest ring in the samples from Bua, which were picked during spring, were originally estimated to be formed a year later than what they actually were. The youngest annual ring of *M. edulis* samples collected in May is hence assumed to be from the previous year. Practically this means that the data in Figure 6 is shifted backwards by a year, as compared to the year of sample collection. To avoid this issue in the future it would be preferable to collect *M. edulis* in the middle of winter, before a new growth ring starts forming. As the nacre forms annual layers parallel to the curvature of the shell, starting on the inner surface of the fibrous layer growing towards the mantle, all annual layers of the nacre can be seen in the umbo region. Furthermore, the nacre is less likely than the fibrous layer to be eroded, as the fibrous layer first has to be fully eroded for the nacre to become exposed. Due to this, annual markings are often easier to identify in the nacre compared to the fibrous layer (Lutz 1976). However, the markings in the nacre cannot be used to locate annual structures in the fibrous layer since, as previously mentioned, the annual markings in the two layers do not align. When studying the annual markings in the nacre, as depicted in the acetate peels, several of the *M. edulis* individuals appear to be between one and two years older than assumed. In conclusion, if a year was missed when dividing the shells according to their external structure, it is difficult to find where it should have been located in the fibrous layer, if the annual marking is only clearly defined in the nacre. In future studies, collecting more shell samples and averaging the result would be preferable.

When re-examining the acetate peels from the Bua 2 and Bua 3 *M. edulis* shells, 11 and 9 annual structures were seen respectively. For comparison, 9 annual structures for Bua 2 and 8 for Bua 3 were identified during the initial sample inspection and preparation. Unfortunately, the imprint of the fibrous layer in the acetate peels was not detailed enough to identify the location of the structures, resulting in it being impossible to tell which in what part of the shell an annual ring has been missed. This does, however, open up for the possibility that the samples assumed to be from 2017 and 2018 from the Bua 2 shell instead being from the same year as the 2016 and 2017 samples from the Bua 3 shell giving an even higher correlation between the sample data (see Figure 6). If, for instance, an annual structure in the young part of the Bua 2 shell has been missed, the later samples will be assumed to be a from a too early date, thus shifting samples by a year. Another possibility is that the aforementioned samples have been mixed during sample preparation. This is deemed to be unlikely as all samples were carefully labeled during each stage of the preparation.

The maximum age of *M. edulis* limits the time span that can be investigated. According to the Norwegian institute of marine research, *M. edulis* can live for 20 years and possibly even longer, and their shells can reach a length of over 10 cm depending on their growth conditions (Havforskningsinstituttet 2024). However, many *M. edulis* individuals do not survive past the first few years of life (McGrorty and Goss-Custard 1993), and it seems reasonable to expect the age of most samples to be less than 20 years.

An alternative to explore for future studies would be to characterize the shell with high-resolution micromilling techniques, combining ^{14}C analysis with measurement of $\delta^{13}C$ and $\delta^{18}O$. The stable isotopes could be used to give information e.g. on water temperature, which could aid to define the annual growth pattern. Time-resolved ^{14}C measurements could reveal discharge patterns from the NPP on a sub-annual basis.

Conclusions

We have evaluated the potential use of annual structures of *M. edulis* shells to estimate past liquid discharges of ^{14}C in the form of DIC from Ringhals nuclear power plant on the Swedish west coast. The approach has proven to be promising but with some challenges, and a few aspects that need further attention.

One challenge is to identify and extract relevant growth structures from the shells. Annual structures appear in the fibrous layer of the shell—which is suitable for ^{14}C analysis—as well as in the nacre, but as these do not align, the nacre needs to be removed. We have found that heating of the shells is efficient to separate the nacre from the fibrous layer. Another challenge, which we believe introduces the main uncertainty within the method, is connected to locating each annual ring within the shell. False annual structures, as well as absent annual structures, may occur in individual mussels. To minimize such effects, several shell samples from each location should be evaluated, instead of individual shells. The method could also be further developed by improving the quality of the acetate peels, and by making growth curves for each sampling location. A further simplification and improvement of the method would be to exclude the acid treatment after the heating step and after cutting the fibrous layer into annual samples.

An advantage of using *M. edulis* shells to retrieve past discharge data is that *M. edulis* is abundant in the area and that they can live up to 20 years. One inherent disadvantage of the approach is that *M. edulis* is semi-sessile, and some individuals may have moved between various habitats during their lifetime. In two shell samples collected at the reference site Särdal in 1978, we observed that $F^{14}C$ in one of the shells agreed well with $F^{14}C$ in *Fucus* spp. from the same site for the period 1974 to 1978. For the other Särdal shell, data agreed well for shell and *Fucus* spp. for 1976–1978, but not for 1972–1975. During these earlier years, this particular individual of *M. edulis* may have resided elsewhere. In two shells collected in 2022 from another reference site, Båteviken, $F^{14}C$ agreed well for both shells and *Fucus* spp. for years 2020–2022. The number of samples from reference sites analyzed within this study are too few to be able to estimate the extent of individuals of *M. edulis* changing habitat, and further investigations are needed. Using several *M. edulis* shells may circumvent the problem, given that changes in habitat are relatively rare.

In this first study of examining the potential of shells of *M. edulis* for retrospective analysis of ^{14}C in the marine environment of Ringhals NPP, we have observed significantly higher $F^{14}C$ values in shells and soft tissue of *M. edulis* from the Ringhals area than from reference sites. Furthermore, $F^{14}C$ varies substantially between years for the Ringhals samples. Despite the uncertainties using shells from *M. edulis* in environmental studies related to liquid discharges from NPPs, we believe that the approach is valuable when other samples from the past are not available.

Supplementary material. To view supplementary material for this article, please visit https://doi.org/10.1017/RDC.2025.10137

Acknowledgment. The project was funded by the Swedish Radiation Safety Authority (SSM), projects SSM2022-4035 and SSM2023-1044-13.

References

Bernhardsson C, Eriksson Stenström K, Jönsson M, Nilsson C and Pédehontaa-Hiaa G (2023) Radiological environmental monitoring at the ESS facility – annual report 2022. *Lund University*. Available at https://portal.research.lu.se/sv/publications/radiological-environmental-monitoring-at-the-ess-facility-annual–5.

Bjarheim S (2024) Can blue mussel shells be used for retrospective ^{14}C-analysis in the marine environment of nuclear power plants? Bachelor thesis. *Lund University*. Available at http://lup.lub.lu.se/student-papers/record/9148362.

Castrillejo M, Witbaard R, Richardson CA, Dekker R, Welte C, Wacker L and Christl M (2020) Impact of nuclear fuel reprocessing on the temporal evolution of marine radiocarbon. *Science of the Total Environment* **738**, 139700.

Checa AG (2018) Physical and biological determinants of the fabrication of molluscan shell microstructures. *Frontiers in Marine Science* **5**, Article 353. doi: 10.3389/fmars.2018.00353.

Clark G (1980) Study of molluscan shell structure and growth lines using thin sections. In Donald CR and Lutz RA (eds), *Skeletal Growth in Aquatic Organisms*. New York: Plenum Press, 603–606.

Conen F, Emmenegger L, Leuenberger M, Steger D and Steinbacher M (2019) ICOS RI, 2020. ICOS ATC ^{14}C release, Jungfraujoch (10.0 m), 2016–01–04–2019–08–12. https://hdl.handle.net/11676/X-lXPKZlO4DWX7wncsLQ7akY; http://calib.org/CALIBomb/. ICOS DATA is licensed under CC4BY (http://creativecommons.org/licenses/by/4.0/).

Cook GT, MacKenzie A, Muir G, Mackie G and Gulliver P (2004) Sellafield-derived anthropogenic ^{14}C in the marine intertidal environment of the NE Irish Sea. *Radiocarbon* **46**, 877–883.

Dunca E and Boalt E (2011) Samband mellan skaltillväxt och ålder hos *Mytilus edulis* i Östersjön blåmusslan [Relation between shell growth and age for blue mussels *Mytilus edulis* in Östersjön]. Rapport Nr 6/2011, Naturhistoriska Riksmuseet Enheten för miljögiftsforskning, Box 50007, 104 05 Stockholm (in Swedish).

Dunca E, Mutvei H, Göransson P, Mörth C-M, Schöne BR, Whitehouse MJ, Elfman M and Baden SP (2009) Using ocean quahog (*Arctica islandica*) shells to reconstruct palaeoenvironment in Öresund, Kattegat and Skagerrak, Sweden. *International Journal of Earth Sciences* **98**, 3–17.

Emmenegger L, Leuenberger M and Steinbacher M (2024) ICOS ATC/CAL ^{14}C Release, Jungfraujoch (5.0 m), 2015–09–21–2022–08–22, ICOS RI. https://data.icos-cp.eu/portal/. ICOS*ATCL2L2–2023.1*JFJ*13.9*779.14C. ICOS DATA is licensed under CC4BY (http://creativecommons.org/licenses/by/4.0/).

Eriksson Stenström K and Mattsson S (2022) Spatial and temporal variations of ^{14}C in *Fucus* spp. in Swedish coastal waters. *Journal of Environmental Radioactivity* **242**, 106794.

Eriksson Stenström K, Skog G, Bernhardsson C, Mattsson S, Nielsen AB, Rundgren M, Muscheler R, Linderson H, Pédehontaa-Hiaa G and Rääf C (2022) Environmental levels of radiocarbon in Lund, Sweden, prior to the start of the European spallation source. *Radiocarbon* **64**(1), 51–67.

Eriksson Stenström K, Skog G, Georgiadou E, Genberg J and Johansson A (2011) A guide to radiocarbon units and calculations. *Lund University*. LUNFD6(NFFR–3111)/1–17/(2011). Available at https://portal.research.lu.se/sv/publications/a-guide-to-radiocarbon-units-and-calculations.

Gillikin DP, Lorrain A, Bouillon S, Willenz P and Dehairs F (2006) Stable carbon isotopic composition of *Mytilus edulis* shells: Relation to metabolism, salinity, δ^{13}C DIC and phytoplankton. *Journal of Organic Geochemistry* **37**(10), 1371–1382.

Gröcke DR and Gillikin DP (2008) Advances in mollusc sclerochronology and sclerochemistry: Tools for understanding climate and environment. *Geo-Mar Lett* **28**, 265–268.

Haag WR and Commens-Carson AM (2008) Testing the assumption of annual shell ring deposition in freshwater mussels. *Canadian Journal of Fisheries and Aquatic Sciences* **65**(3), 493–508.

Hammer S and Levin I (2017) Monthly mean atmospheric Δ^{14}CO2 at Jungfraujoch and Schauinsland from 1986 to 2016. Available at https://doi.org/10.11588/DATA/10100, heiDATA, V2.

Havforskningsinstituttet (2024) Tema: Blåskjell. Available at https://www.hi.no/hi/temasider/arter/blaskjell (Updated: 3rd of December 2024. Accessed: 4th of March 2025) (in Norwegian).

International Atomic Energy Agency (IAEA) (2004) Management of waste containing tritium and carbon-14. *Technical Report Series No. 421*.

Kautsky N (1982) Growth and size structure in a Baltic *Mytilus edulis* population. *Marine Biology* **68**, 117–133.

Kennish MJ (1980) Preparation of acetate peels and fractured sections for observation of growth patterns within the bivalve shell. In Rhoads CR and Lutz RA (eds), *Skeletal Growth of Aquatic Organisms*. New York: Plenum Press, 597–601.

Levin I and Kromer B (2004) The tropospheric $^{14}CO_2$ level in mid latitudes of the northern hemisphere (1959–2003). *Radiocarbon* **46**, 1261–1271.

Levin I, Kromer B and Hammer S (2013) Atmospheric $\Delta^{14}CO_2$ trend in western European background air from 2000 to 2012. *Tellus B: Chemical and Physical Meteorology* **65**(1), 20092.

Ljunghager F (2017) Blåmussla. *Havs- och vattenmyndigheten*. Available at https://www.havochvatten.se/arter-och-livsmiljoer/arter-och-naturtyper/blamussla.html (Accessed: 8 September 2024).

Lougheed BC, Filipsson HL and Snowball I (2013) Large spatial variations in coastal ^{14}C reservoir age – a case study from the Baltic Sea. *Climate of the Past* **9**(3), 1015–1028.

Lutz RA (1976) Annual growth patterns in the inner shell layer of *Mytilus edulis*. *Journal of the Marine Biological Association of the United Kingdom* **56**(3), 723–731.

Magnusson Å (2007) ^{14}C produced by nuclear power reactors – generation and characterization of gaseous, liquid and solid waste. PhD dissertation. *Lund University*.

Magnusson Å, Aronsson P-O, Lundgren K and Stenström K (2008a) Characterization of ^{14}C in Swedish light water reactors. *Health Physics* **95**(2), S110–S121.

Magnusson Å, Stenström K and Aronsson P (2008b) ^{14}C in spent ion-exchange resins and process water from nuclear reactors: A method for quantitative determination of organic and inorganic fractions. *Journal of Radioanalytical and Nuclear Chemistry* **275**(2), 261–273.

Mattsson S, Eriksson Stenström K and Pédehontaa-Hiaa G (2022) Long-time variations of radionuclides and metals in the marine environment of the Swedish west-coast studied using brown algae (*Fucus serratus* and *Fucus vesiculosus*). Report SSM 2022:13. *Swedish Radiation Safety Authority*. Available at www.ssm.se.

Mattsson S, Eriksson Stenström K, Pédehontaa-Hiaa G, Bernhardsson C, Jönsson M, López-Gutiérrez JM, Lérida-Toro V and Chamizo Calvo E (2025) Radionuclides in algae from Swedish coastal waters for over half a century. *Radiation Protection Dosimetry* **201**(13–14), 974–994.

McGrorty S and Goss-Custard JD (1993) Population dynamics of the mussel *Mytilus edulis* along environmental gradients: Spatial variations in density-dependent mortalities. *Journal of Animal Ecology* **62**(3), 415–427.

Millstein J and O'Clair CE (2001) Comparison of age-length and growth-increment general growth models of the Schnute type in the Pacific Blue Mussel, *Mytilus trossulus* Gould. *Journal of Experimental Marine Biology and Ecology* **262**(2), 155–176.
Neves RJ and Moyer SN (1988) Evaluation of techniques for age-determination of freshwater mussels (*Unionidae*). *American Malacological Bulletin* **6**(2), 179–188.
OSPAR Commission (2024) Available at https://www.ospar.org/work-areas/rsc (Accessed: 19 August 2024).
Qiao J, Andersson K and Nielsen S (2020) A 40-year marine record of ^{137}Cs and ^{99}Tc transported into the Danish Straits: Significance for oceanic tracer studies. *Chemosphere* **244**, 125595.
Qiao J, Zhang H, Steier P, Hain K, Hou X, Vartti V-P, Henderson GM, Eriksson M, Aldahan A, Possnert G and others (2021) An unknown source of reactor radionuclides in the Baltic Sea revealed by multi-isotope fingerprints. *Nature Communications* **12**(1), 823.
Reimer PJ, Baillie MG, Bard E, Bayliss A, Beck JW, Blackwell PG, Ramsey CB, Buck CE, Burr GS and Edwards RL (2009) IntCal09 and Marine09 radiocarbon age calibration curves, 0–50,000 years cal BP. *Radiocarbon* **51**(4), 1111–1150.
Reimer PJ, Brown TA and Reimer RW (2004) Discussion: Reporting and calibration of post-bomb ^{14}C data. *Radiocarbon* **46**(3), 1299–1304.
Schöne BR, Fiebig J, Pfeiffer M, Gleß R, Hickson J, Johnson AL, Dreyer W and Oschmann W (2005) Climate records from a bivalved Methuselah (*Arctica islandica*, Mollusca; Iceland). *Palaeogeography, Palaeoclimatology, Palaeoecology* **228**(1–2), 130–148.
Scourse JD, Wanamaker AD, Weidman C, Heinemeier J, Reimer PJ, Butler PG, Witbaard R and Richardson CA (2012) The marine radiocarbon bomb pulse across the temperate North Atlantic: A compilation of δ^{14}C time histories from *Arctica islandica* growth increments. *Radiocarbon* **54**(2), 165–186.
Seed R (1969) The ecology of *Mytilus edulis* L. (Lamellibranchiata) on exposed rocky shores. II. Growth and mortality. *Oecologia* **3**(3/4), 317–350.
Seed R (1980) Chapter 1: Shell growth and form in the Bivalvia. In Rhoads CR and Lutz RA (eds), *Skeletal Growth of Aquatic Organisms*. New York: Plenum Press, 23–61.
Skog G (2007) The single stage AMS machine at Lund University: Status report. *Nuclear Instruments and Methods in Physics Research Section B: Beam Interactions with Materials and Atoms* **259**(1), 1–6.
Skog G, Rundgren M and Sköld P (2010) Status of the single stage AMS machine at Lund University after 4 years of operation. *Nuclear Instruments and Methods in Physics Research Section B: Beam Interactions with Materials and Atoms* **268**(7–8), 895–897.
Skoglund P-O and Peterson C (1988) Ringhals – Kylvattenutsläpp i havet. Slutrapport från oceanografiska undersökningar utaför Ringhals kärnkraftverk med fyra aggregat i drift. *SMHI Oceanografi*, Nr 25. (In Swedish).
Smaal AC and Vonck A (1997) Seasonal variation in C, N and P budgets and tissue composition of the mussel *Mytilus edulis*. *Marine Ecology Progress Series* **153**, 167–179.
Spötl C, Mattey D (2006) Stable isotope microsampling of speleothems for palaeoenvironmental studies: A comparison of microdrill, micromill and laser ablation techniques. *Chemical Geology* **235**(1–2), 48–58.
SSMFS (2021) Strålsäkerhetsmyndighetens föreskrifter och allmänna råd om drift av kärnkraftsreaktorer [The radiation safety authority's regulations and general advice regarding nuclear reactors]. *Strålsäkerhetsmyndigheten.* (In Swedish).
Steinhardt J, Butler PG, Carroll MJ and Hartley J (2016) The application of long-lived bivalve sclerochronology in environmental baseline monitoring. *Frontiers in Marine Science* **3**, Article 176.
Stenström K, Skog G, Nilsson CM, Hellborg R, Leide-Svegborn S, Georgiadou E and Mattsson S (2010) Local variations in ^{14}C – How is bomb-pulse dating of human tissues and cells affected? *Nuclear Instruments and Methods in Physics Research Section B: Beam Interactions with Materials and Atoms* **268**(7–8), 1299–1302.
Surge DM and Schöne BR (2013) Bivalve sclerochronology. In *Encyclopedia of Scientific Dating Methods*. *Springer Science+Business Media Dordrecht*. doi: 10.1007/978-94-007-6326-5_165-1.
Tierney KM (2017) Marine ecosystem uptake of nuclear reprocessing derived radiocarbon (^{14}C). PhD dissertation. University of Glasgow.
United Nations Scientific Committee on the Effects of Atomic Radiation (UNSCEAR) (2016) UNSCEAR 2016 report—sources, effects and risks of ionizing radiation. Report to the General Assembly. Scientific Annexes A, B, C, and D.
Wacker L, Němec M and Bourquin J (2010) A revolutionary graphitisation system: Fully automated, compact and simple. *Nuclear Instruments and Methods in Physics Research Section B: Beam Interactions with Materials and Atoms* **268**(7–8), 931–934.
Wurster CM, Patterson WP and Cheatham MM (1999) Advances in micromilling techniques: A new apparatus for acquiring high-resolution oxygen and carbon stable isotope values and major/minor elemental ratios from accretionary carbonate. *Computers and Geosciences* **25**(10), 1159–1166.
Zuykov M and Schindler M (2019) Sclerochronology-based geochemical studies of bivalve shells: Potential vs reality. *Estonian Journal of Earth Sciences* **68**, 37–44.

Cite this article: Bjarheim S, Eriksson Stenström K, Lindskog A, Olsson M, Carlsson P, and Mattsson S. The potential of shells from *Mytilus edulis* for retrospective analysis of marine ^{14}C discharges from nuclear power plants. *Radiocarbon* 1–16. https://doi.org/10.1017/RDC.2025.10137